研 究 解 説

New X-cut Lithium Niobate Optical Modulator with Velocity and Impedance Matching

新しい速度・位相整合法を用いたXカットニオブ酸リチウム光変調器

Ales FILIP* and Yoichi FUJII*
アレシュ フィリップ・藤 井 陽 一

New x_c-cut, y_c-propagating lithium niobate optical modulators with simultaneous phase velocity and impedance matching are presented and numerically analyzed. It is found that ridge optical waveguides placed between thick coplanar travelling wave electrodes enable to match microwave effective index to 2.1 and electrode characteristic impedance to 50 Ω. Three configurations are proposed. In the first, the electrodes are supported by silicon oxide buffer layer in the grooves between ridge regions. In the second and third, the electrodes are plated either on the lower or upper part of thin membrane with high resistivity and low dielectric permittivity. Numerical results show that when the membrane supports thick electrodes, the best device performance of 3-dB electrical bandwidth exceeding 144 GHz and 6.4 V driving voltage can be obtained.

1. Introduction

The use of external modulators in fast communication, computer and signal processing systems requires a modulation bandwidth exceeding several tens of gigahertz and a low driving voltage which make it compatible with other low-voltage driven electronics. The lithium niobate traveling wave modulator is one of the promising candidates for these broadband applications[1)~6),9),13),17),18)].

This paper presents a new approach to the design of broadband x_c-cut, y_c-propagating lithium niobate optical modulators under simultaneous conditions of phase velocity and impedance matching. Three different types of modulators are proposed and numerically investigated. The first modulator employs a silicon oxide buffer layer in the grooves outside the ridge regions for supporting the thick coplanar traveling wave electrodes. In the other two types, the thick electrodes are plated either on the lower or on the upper part of a thin membrane of high resistivity and low dielectric permittivity.

In this paper, a ridge *xc*-cut, *yc*-propagating lithium niobate optical modulator structures with traveling wave electrodes placed between ridge optical waveguides are presented. We describe phase velocity and characteristic impedance matching techniques based on replacing the high dielectric permittivity material in the regions outside the optical waveguides by a low dielectric permittivity material. The microwave effective index ($Nm=(\varepsilon eff)^{1/2}$) is therefore reduced considerably while the characteristic Z_o impedance is increased. This idea is common to all three proposed modulators and it is the fundamental step for matching. Further improvement is achieved by an appropriate design of the electrode structures. These electrode structures can be applied for both phase and intensity modulation. In the case of intensity modulation, the arms of the Mach-Zehnder interferometer are placed between the electrodes as described earlier for the case of common plane x_c-cut modulators.

The main modulator parameters, such as the microwave effective index, the characteristic impedance, the conductor attenuation coefficient and the half-wave voltage electrode length product, are analyzed by using the finite element method (FEM)[16),19)] which is applicable for analyzing structures with arbitrary shape and arbitrary number of electrodes and materials. Inhomogeneous regions are approximated by a number of homogeneous subregions. Since the lithium niobate is an anisotropic dielectric material, two components of the dielectric permittivity

* Department of Electrical Engineering and Electronics, Institute of Industrial Science, University of Tokyo

tensor ε must be used in each subregion. The analysis is based on a quasi-TEM approach because the wavelength of the applied electromagnetic fields is much larger than the crossection dimensions and the dispersion can be neglected[10]. The characteristic impedance Z_o, the microwave effective index N_m and the conductor attenuation coefficient α_c are calculated directly from the strength of the electric field. The driving voltage is determined by using an overlap integral[11]. For this purpose, the electric field of the light in the optical waveguides is approximated by Hermite-Gaussian function[8]. The calculations were carried out for all three proposed structures and the theoretical bandwidth was determined.

2. Matching Techniques and Proposed Structures

Generally, the microwave effective index N_m of traveling wave electrodes directly plated on an x-cut lithium niobate substrate, depends on the structure dimensions, and is about 4.2[7]. The microwave effective index can be reduced to approximately 3.2 by using a 1 μm silicon oxide buffer layer. Since the difference between the electrical and the optical phase velocities of the structure is directly proportional to the difference between the microwave effective and optical refractive indices, the modulator bandwidth, which is limited by the transit-time factor, can be expressed by a well known formula[12],

$$f_{max}[-3 \text{ dB electrical}] = 1.4 \ c \ / \ \{\pi L \ (Nm-No)\}$$

where c is the velocity of light in the vacuum, L is the length of the modulator and N_m and N_o are the microwave effective and optical refractive indices, respectively. For instance, if the modulator length L is 25 mm, and the optical index of refraction No is 2.1, then about a 5.3 GHz electrical bandwidth can be obtained. For index differences (N_m-N_o) 0.1 and 0.05, respective bandwidths of 53 and 106 GHz are obtained.

The second limiting factor of a modulator bandwidth is the microwave electrode attenuation which is mainly caused by frequency dependent losses. The frequency dependent loss consists of losses in the dielectric material and losses due to skin effect. The dielectric loss in high resistivity dielectric materials is much smaller than losses caused by the skin effect and can therefore be neglected. The latter component can be expressed as $\alpha_c=\alpha_o(f)^{1/2}$, where α_o depends on the conductivity of the materials, crossection dimensions and other parameters of the structure. The electrode crossection dimensions have to be small enough to limit phase velocity dispersion and, on the other hand, be sufficiently large to reduce conductor losses. Moreover, the driving voltage of a structure is usually required to be as low as possible. As will be shown in the next subsections, the solution can be found in an appropriate configuration of the optical waveguides and the traveling wave electrodes. Note that throughout this paper we use electrical bandwidth rather than the optical bandwidth (−3 dB optical = −6 dB electrical).

A. Electrodes Supported by Buffer Layer

The first proposed structure is shown in Fig. 1. In the regions under the central and ground electrodes a relatively large volume of lithium niobate with high relative dielectric permittivity tensor components ($\varepsilon_{rx}=28$, $\varepsilon_{ry}=43$) is replaced by a silicon oxide buffer layer which has a low dielectric constant ($\varepsilon_r=4$). Compared with the structure whose electrodes are directly plated on a lithium niobate substrate, a larger proportion of the electromagnetic energy is now propagating in air. The microwave effective index is therefore lower and the impedance higher.

Additional increase in the microwave velocity and characteristic impedance can be achieved by inserting a gap G between the central electrode and the ridge. If the gap G is widened, the microwave effective index Nm becomes smaller and the characteristic impedance goes up. The microwave effective index is now reduced because the electromagnetic field propagates beside the lithium niobate crystal within a low dielectric permittivity material. The

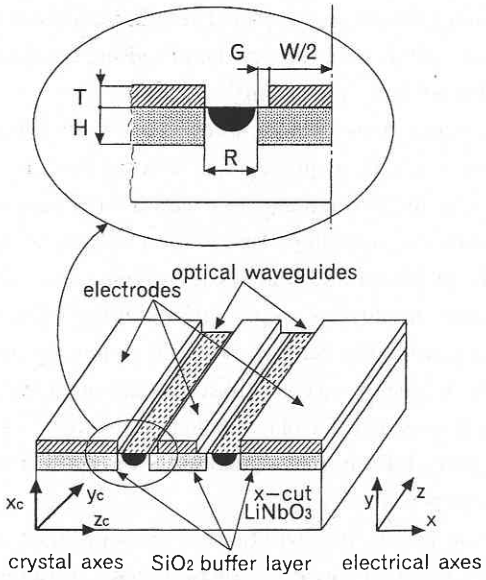

Fig. 1 Integrated-optic realization of the ridge modulator on xc-cut, yc-propagating lithium niobate substrate with electrodes plated on silicon oxide buffer layer.

characteristic impedance Z_o increases as a result of a smaller capacitance between the electrodes which is caused both by a wider electrode gap ($R+G$) and the lower permittivity of the material in which the electromagnetic waves propagate. Since the half-wave voltage electrode length product ($V_\pi L$) is to be low, the electrode gap ($R+G$) should be made as narrow as possible.

However, the minimum dimensions of R and G are determined by the phase velocity and characteristic impedance matching conditions and the minimum width of the ridge R is further limited by the minimal transverse dimension of the optical waveguide. In the case of intensity modulator, Mach-Zehnder interferometer is introduced and a push-pull effect utilized. The crosstalk between the two arms of the Mach-Zehnder interferometer, which depends on the optical waveguide configuration and structure dimensions, should not exceed a specified level and this parameter should also be taken into account in the modulator design and choice of parameters size.

The design of a traveling wave electrode with a low conductor attenuation coefficient α_c and thus an extended modulator bandwidth can be achieved by increasing the electrode thickness. If the electrode thickness T is increased, a larger proportion of the microwave power propagates in the air and therefore the microwave effective index is reduced.

On the other hand, if the central electrode is made wider, the microwave effective index N_m increases, because the electromagnetic waves propagate to a larger extent in higher permittivity material. Larger crossection dimensions (T, W) mean a greater electrode capacitance or, in turn, a smaller impedance Z_o. Usually, in modulator design, one wants to decrease the microwave effective index N_m as closely as possible to the optical index of refraction N_o (e.g. to 2.1 at optical wavelength $\lambda = 1.3$ μm) and at the same time increase the characteristic impedance Z_o to approximately 50 Ω.

If the requirement of a broad-band and low-driving voltage operating regime is added, then the conditions for this regime and the conditions for phase velocity and impedance matching contradict. Therefore, the key to the solution is in the electrode structure geometry.

It should be noted that for the sake of simplicity open optical ridge waveguides are considered in this and the next two subsections. In practice, these regions should be covered by a thin silicon oxide buffer layer to reduce optical loss. This low dielectric permittivity layer has a small effect on the above shown electrical parameters and this effect can be compensated by slight variations of the geometrical dimensions of the structure.

B. Electrodes on the Lower Part of a Membrane

An application of the modified membrane supported transmission line structure[14),15)] for a broadband optical modulator is shown in Fig. 2(a). As in the previous case, the modulator structure employs x_c-cut, y_c-propagating lithium niobate substrate with ridge optical waveguides. Instead of the supporting silicon oxide buffer layer, the travelling wave electrode is suspended from a thin membrane in such a way, that the electrode is placed between the ridge regions. The phase velocity and impedance matching is then obtained by two gaps: one air gap H is between the membrane with the electrodes and the lithium niobate substrate and another gap G is between the ridge regions and central electrode. The electromagnetic field propagates mainly in the area between the electrodes and in the ridge regions which include the optical waveguides, where an electrooptical phase shift is to be induced.

A smaller microwave effective index N_m and conductor attenuation coefficient α_c can also be achieved by a thick electrode. In this case, employing a ditch membrane, which is shown in Fig. 2(b), seems advantageous. Removing the

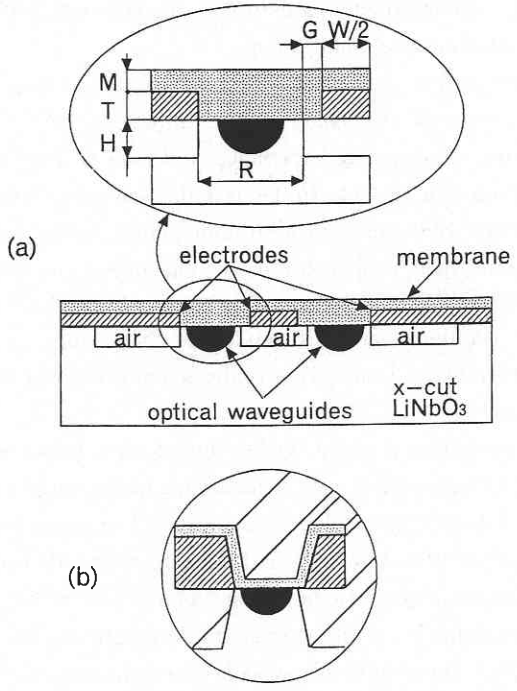

Fig. 2 *Xc*-cut ridge lithium niobate optical modulator with electrodes on the lower part of the membrane.
(a) intensity modulator with plane membrane,
(b) detail of ditch membrane.

dielectric material from the region between the electrodes decreases the microwave effective index and the characteristic impedance is increased. Moreover, the conductor loss is also reduced. On the other hand it should be noted that the fabrication process becomes more complicated.

C. Electrodes on the Upper Part of a Membrane

In the other possible design of x_c-cut ridge lithium niobate broadband optical modulator the electrode structure is supported by a thin dielectric membrane. The proposed structure is shown in Fig. 3(a). Unlike the previously suggested structure, the thin plane membrane is directly placed on the top of the ridge regions containing the optical waveguides, and the central traveling wave electrode is plated on its upper surface between the ridge regions. This structure differs, from the previous one, in that no dielectric is present between the side walls of the central and ground electrodes.

Phase velocity and impedance matching is achieved by inserted air gap (W) between the ridges and a vertical gap between the electrodes and the active lithium niobate material. The latter is determined by the membrane thickness (M). The relative configuration of the lithium niobate substrate, the membrane and the electrodes results in better confinement of the propagating field within the active regions containing optical waveguides rather than in the othe'nonfunctional' areas.

This greatly reduces the microwave effective index N_m and increases the characteristic impedance Z_o. Simultaneous velocity and impedance matching is more easily achieved with thick electrodes as in the previously described structure. Since in such a structure much of the electromagnetic field propagates in the air rather than in the lithium niobate substrate, the conductor loss, which is the main limiting factor of modulator bandwidth, is also considerably reduced. This is the main advantage of this structure.

A modification of this type of modulator is shown is Fig. 3(b). In the modified case, a membrane with a ridge shape is used rather than a plane membrane. The membrane is supported at both the top and the trapezium side walls of the lithium niobate ridge region. As a matter of fact, this configuration is a combination of the structures in Fig. 1 and Fig. 3(a). The membrane partially covers the trapezium side walls in the optical waveguide regions but at the same time an air gap is kept between the membrane and the substrate, which is the advantage of the structure in Fig. 3(a). The main reason for employing such a shape for the membrane

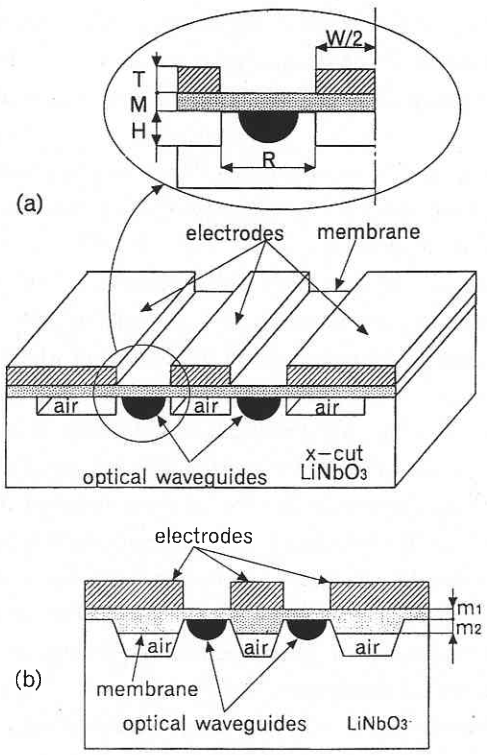

Fig. 3 *Xc*-cut ridge lithium niobate optical modulator with electrodes on the upper part of the membrane.
(a) intensity modulator with plane membrane,
(b) intensity modulator with ridge membrane.

is to increase the strength of the driving electromagnetic field in the optical waveguide regions which enables to decrease the driving voltage. In this case, velocity and impedance matching is easily obtained by optimization the membrane parameters m_1 and m_2 (see Fig. 3(b)).

All the above proposed modulator structures were analyzed and the effects of the buffer layer thickness H, ridge width R, gap G between ridge and electrode, electrode thickness T and width W, membrane thickness M were investigated.

3. Numerical Results

A. Electrodes Supported by Buffer Layer

First, we investigated the modulator with electrodes plated on the buffer layer as described in II.A. The dependances of the microwave effective index, characteristic impedance, conductor attenuation coefficient and half-wave voltage electrode length product on the modulator dimensions were numerically simulated. At first we studied the effect of varying the buffer layer thickness H. From Fig. 1 we can see, that the buffer layer thickness H is the same as

the height of the ridge. The relative dielectric constant $\varepsilon_{rb} = 4$ was taken as that of the silicon-oxide buffer. By employing a silicon oxide buffer layer (4 μm), a characteristic impedance of 42 Ω and a microwave effective index of 3.3 were achieved.

For a larger microwave phase velocity and higher characteristic impedance, a gap G between the ridge and the central electrode was introduced. The calculated characteristic impedance Z_o and the effective index N_m as a function of the width of the gap G are shown in Fig. 4.

The ridge width R is taken as a parameter. For instance, for a ridge width R of 10 μm, a gap G of 0.6 μm, an electrode thickness T of 2 μm and width W of 8 μm, a characteristic impedance of 56 Ω and a microwave effective index of 2.3 were calculated. The characteristic impedance becomes higher than specified. The corresponding driving voltage for a modulator of length L = 25 mm is about 4.8 V. The effect of the electrode thickness is shown in Fig. 5(a), where the ridge width R is still a parameter. Thicker electrodes make the driving electromagnetic field propagated in the air space rather than in the high permittivity region. From the chart we can see that for a gap G of 1 μm, a ridge width R of 14 μm and a conductor thickness T of 6 μm, a microwave effective index N_m of 2.15 and characteristic impedance Z_o of 56 Ω are achieved.

The effect of varying the electrode thickness for various gap size G is shown in Fig. 5(b). In this case, the impedance and the velocity matched structure N_m=2.12, Zo=49 Ω can be obtained by a gap G of 0.6 μm, a ridge width R of 10 μm, an electrode width W of 8 μm and a thickness T of 6 μm. In the modulator design, the electrode width W is an important parameter, which mainly influences the characteristic impedance and the conductor attenuation coefficient. These effects what will be shown in the evaluation of an example of the third structure (Fig. 3(a)).

B. Electrodes on the Lower Part of a Membrane

The modulator with electrodes plated on the lower part of thin membrane is shown in Fig. 2(a). From the figure one can assume, that the electromagnetic field is guided mainly in the active regions between the central and ground electrodes and in the dielectric membrane. The air gap H in the ridge area reduces the capacitance of the electrode structure, which results in a smaller microwave effective index N_m and a larger the characteristic impedance Z_o.

Fig. 6 shows the dependence of the characteristic impedance Z_o and the microwave effective index N_m as a function of the gap G between the ridge and the central

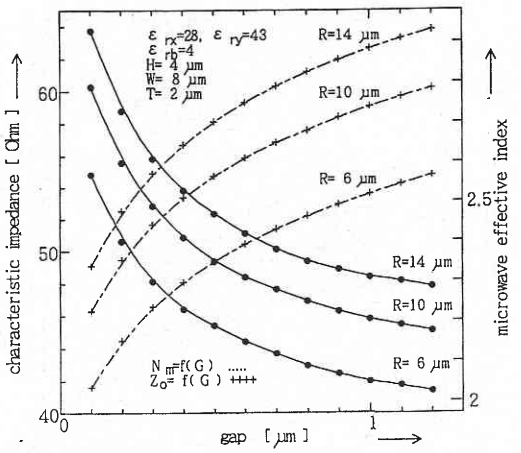

Fig. 4 Characteristic impedance Zo and microwave effective index Nm as a function of gap width G, ridge width R is parameter. Buffer layer thickness H=4 μm, electrode width and thickness W=8 μm and T=2 μm, εrx=28, εry=43 and εrb=4.

electrode. For instance, if the structure has a gap G of 0.4 μm, an electrode of width 8 μm and thickness 4 μm, and a ridge height H of 3 μm, the microwave effective index N_m becomes close to 2.17 and the characteristic impedance to 54 Ω. The impedance can be easily reduced to 50 Ω by widening the central electrode. Since the membrane dielectric constant ε rm and thickness M are low, the change in the microwave effective index N_m will be small.

The half-wave voltage active electrode length product $V_\pi L$, and the conductor attenuation coefficient as a function of the gap G, are shown in Fig. 7. The electrode thickness T is a parameter. From this chart it is clear that the conductor loss is higher than for the previous structure. This is caused by the wrapping of the electrodes from the upper side by the membrane. It is calculated that a velocity and impedance matched modulator (R=10 μm, M=2 μm, H=3 μm, W=8 μm, G=0.4 μm, L=25 mm) in a Mach-Zehnder configuration has a driving voltage of 6.5 V.

C. Electrodes on the Upper Part of a Membrane

The structure under consideration is shown in Fig. 3(a). The electrodes are plated directly on the upper side of a thin membrane, so compared to the structure in the Fig. 2(a), the electromagnetic field penetrates deeper into the air because of the absence of a dielectric in the region between the electrode sidewalls. The horizontal gap between the central electrode and the ridge (Fig. 2(a)) is replaced by a space due to the membrane thickness M. As a result the microwave effective index N_m can be easily matched to the optical index of refraction N_o, the impedance can be easily increased to 50 Ω and the conductor attenuation coefficient

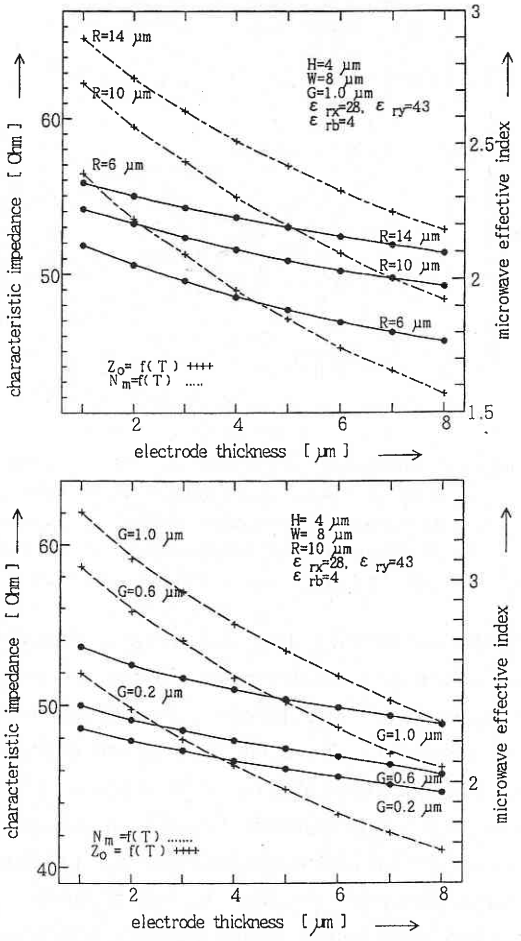

Fig. 5 Characteristic impedance Zo and microwave effective index Nm as a function of electrode thickness T. Buffer layer thickness H=4 μm, electrode width W=8 μm, εrx=28, εry=43 and εrb=4.
(a) ridge width R is parameter: gap G=1 μm,
(b) gap G is parameter: R=10 μm.

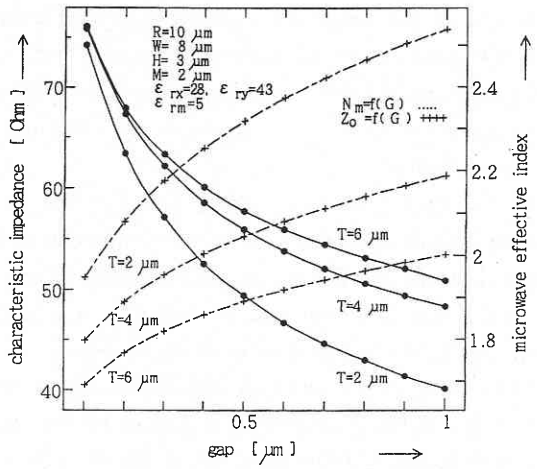

Fig. 6 Characteristic impedance Zo and microwave effective index Nm as a function of gap G, electrode thickness T is parameter. Ridge width R=10 μm, electrode width W=8 μm, ridge height H=3 μm, membrane thickness M=2 μm, εrx=28, εry=43 and εrm=5.

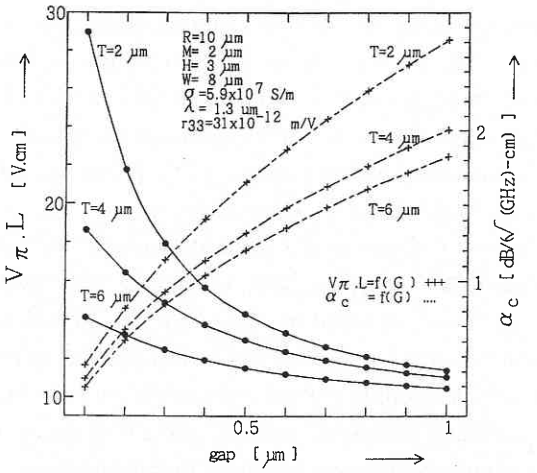

Fig. 7 Half-wave voltage electrode length product $V\pi L$ and conductor attenuation coefficient αc as a function of gap G, electrode thickness T is parameter. Ridge width R=10 μm, membrane thickness M=2 μm, ridge height H=3 μm, electrode width W=8 μm, εrx=28, εry=43 and εrm=5.

α c can be reduced.

Fig. 8 shows the dependence of the characteristic impedance Z_o and the microwave effective index N_m as a function of the membrane thickness M, where the electrode thickness T is taken as the parameter. For example, for a membrane thickness of 1 μm, which is technically reasonable, and a ridge width R of 10 μm and height H of 3 μm, an electrode thickness T of 6 μm and width W of 10 μm, a characteristic impedance of 48.5 Ω and N_m close to 2.0 are achieved.

Fig. 9 shows the dependence of the characteristic impedance Z_o and the microwave effective index N_m as a function of the ridge width R. The electrode thickness T is again a parameter. From the graph we can see that Z_o is matched to 50 Ω and Nm to 2.1 for a ridge width R of 12 μm, electrode thickness T of 6 μm and width W of 10 μm and ridge height H of 3 μm.

Since the propagation of the electromagnetic field is limited to a relatively small subregion with a high dielectric permittivity, the conductor loss is reduced considerably and this structure has the lowest conductor attenuation coefficient of all the three proposed modulators. For a velocity

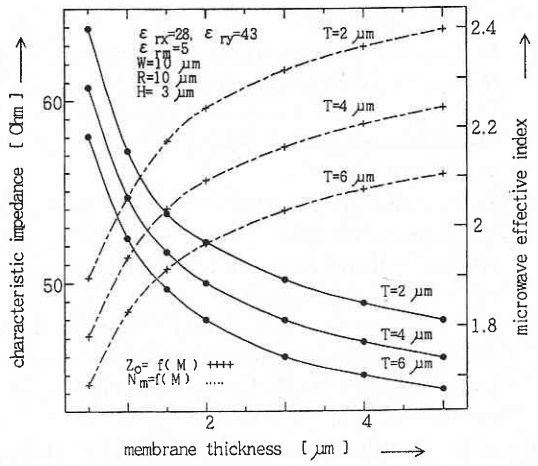

Fig. 8 Characteristic impedance Zo and microwave effective index Nm as a function of membrane thickness M, electrode thickness T is parameter. Electrode width W=10 μm, ridge width R=10 μm, ridge height H=3 μm, εrx=28, εry=43 and εrm=5.

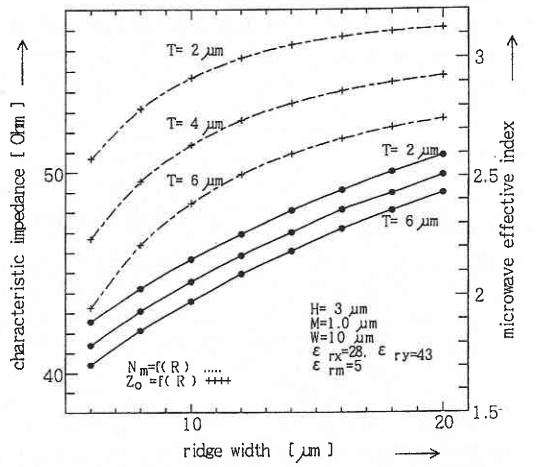

Fig. 9 Characteristic impedance Zo and microwave effective index Nm as a function of ridge width R, electrode thickness T is parameter. Ridge height H=3 μm, membrane thickness M=1 μm, electrode width W=10 μm, εrx=28, εry=43 and εrm=5.

and impedance matched structure (H=3 μm, W=10 μm, R=12 μm, T=6 μm, M=1 μm, and L=25 mm) a conductor attenuation coefficient less than 0.1 dB/((GHz)1/2−cm) is achieved which extends the theoretical electrical bandwidth to beyond 144 GHz. A 6.4 V driving voltage is calculated.

4. Conclusion

In this paper, the characteristic impedance and phase velocity matched x-cut lithium niobate optical modulators were presented and three structures were numerically analyzed. All the proposed modulators employ a ridge lithium niobate structure and differ in the configuration of the travelling wave electrodes. The results show that for modulator length of 25 mm, the best performance can be achieved by a structure based on a coplanar thick electrodes plated on the upper part of thin membrane. Under velocity and impedance matching conditions a 6.4 V driving voltage and a conductor attenuation coefficient less than 0.1 dB/((GHz)1/2-cm) can be obtained, which corresponds to an electrical bandwidth of 144 GHz. This performance is better than that of the structure whose electrodes are directly plated on the buffer layer (36 GHz electrical bandwidth). In practice, the conductor losses of a real device will be higher because of various fabrication imperfectness, discontinuities and other effects but it is expected that such a modulator structure could be a potential candidate for application in 100 Gb/s communication systems.

Acknowledgment

The authors would like to thank A. Levanon for his helpful remarks. (Manuscript received, December 5, 1995)

References

1) K. Noguchi, K. Kawano, T. Nozawa and T. Suzuki, "A Ti:$LiNbO_3$ Optical Intensity Modulator with More Than 20 GHz Bandwidth and 5.2 V Driving Voltage," IEEE Photon. Technol. Lett., vol.3, pp. 333–335, 1991.
2) D. W. Dolfi and T. R. Ranganath, "50 GHz Velocity-Matched Broad Wavelength $LiNbO_3$ Modulator with Multimode Active Section," Electron. Lett., 1992, 28, pp. 1197–1198.
3) G. K. Gopalakrishnan, C. H. Bulmer, W. K. Burns, R. W. McElhanon and A. S. Greenblatt, "40 GHz, Low Half-wave Voltage Ti:$LiNbO_3$ Intensity Modulator, Electron. Lett., 1993, vol. 28, pp. 826–827.
4) K. Noguchi and K. Kawano, "Proposal Ti: $LiNbO_3$ Optical Modulator with Modulation Bandwidth of More Than 150 GHz," Electron. Lett., 1992, 28, pp. 1759–1761.
5) K. Noguchi, O. Mitomi, K. Kawano and M. Yanagibashi, "Highly Efficient 40-GHz Bandwidth Ti:$LiNbO_3$ Optical Modulator Employing Ridge Structure," IEEE Photon. Technol. Lett., vol. 5, pp. 52–54, 1993.
6) K. Noguchi, H. Miyazawa and O. Mitomi, "75 GHz Broadband Ti:$LiNbO_3$ Optical Modulator with Ridge Structure," Electron. Lett., 1994, 30, pp. 949–951.
7) H. Jin, M. B'elanger and Z. Jakubczyk, "General Analysis of Electrodes in Integrated-Optics Electrooptic Devices," IEEE J. Quantum Electron., QE-27, pp. 243–251, Feb. 1991.

8) R. A. Becker and B. E. Kincaid, "Improved Electrooptic Efficiency in Guided-Wave Modulators," IEEE J. Lightwave Technol., vol. 11, pp. 2076–2079, Dec. 1993.
9) R. L. Jungerman, D. W. Dolfi, "Frequency Domain Optical Network Analysis Using Integrated Optics," IEEE J. Quantum Electron., vol. QE-27, pp. 580–587, March 1991.
10) T. Kitazawa, D. Polifko and H. Ogawa, "Analysis of CPW for $LiNbO_3$ Optical Modulator by Extended Spectral-Domain Approach," IEEE Microwave and Guided Wave Lett., vol. 2, pp. 313–315, August 1992.
11) C. M. Kim, R. V. Ramaswamy, "Overlap Integral Factors in Integrated Optic Modulators and Switches," J. Lightwave Technol., vol. 7, pp. 1063–1070, July 1989.
12) H. Chung, W. S. C. Chang and E. L. Adler, "Modeling and Optimization of Traveling-Wave $LiNbO_3$ Interferometric Modulators," IEEE J. of Quantum Elect., vol. 27, pp. 608–617, March 1991.
13) H. Chung, W. S. C. Chang and G. E. Betts, "Microwave Properties of Traveling-Wave Electrode in $LiNbO_3$ Electrooptic Modulators," IEEE J. Lightwave Technol., vol. 11, pp. 1274–1278, August 1993.
14) L. P. B. Katehi, G. M. Rebeiz, T. M. Weller, R. F. Drayton, H. J. Cheng and J. F. Whitaker, "Micromachined Circuits for Millimeter- and Sub-millimeter-Wave Application," IEEE Antennas and Propagation Magazine, vol. 35, pp. 9–17, Oct. 1993.
15) H. Cheng, J. F. Whitaker, T. M. Weller, and L. P. B. Katehi, "Terahertz-Bandwidth Pulse Propagation on a Coplanar Stripline Fabricated on a Thin Membrane," IEEE Microwave and Guided Wave Lett., vol. 4, pp. 89–91, March 1994.
16) Z. P. Pantic and R. Mittra, "Quasi-TEM Analysis of Microwave Transmission Line by the Finite Element Method, " IEEE Trans. Microwave Theory Tech., vol. MTT-34, pp. 1096–1103, Nov. 1986.
17) E. L. Wooten and S. C. Chang, "Test Structures for Characterization of Electrooptic Waveguide Modulators in Lithium Niobate," IEEE J. Quantum Electron., vol. 29, , pp. 161–170, Jan. 1993.
18) G. K. Gopalakrishnan, W. K. Burns and C. H. Bulmer, "Electrical Loss Mechanism in Travelling Wave $LiNbO_3$ Optical Modulators," Electron. Lett., 1992, 28, pp. 207–208.
19) P. P. Silvester and R. L. Ferrari, Finite Elements for Electrical Engineers, 2 nd edition. Cambridge: Cambridge University Press, 1990.
20) J. Jin, The Finite Element Method in Electromagnetic. New York: John Wiley Sons, Inc, 1993.
21) J. E. Akin, Finite Elements for Analysis and Design. London: Academic Press, 1994.